TECHNICAL RESEARCH REPORT

Institute for Systems Research

A Rotary Magnetostrictive Motor for Robotics

by C.A. Teolis and J. Loncaric

The Institute for Systems Research is supported by the National Science Foundation Engineering Research Center Program (NSFD CD 8803012), Industry and the University

TR 93-27

A Rotary Magnetostrictive Motor for Robotics

Carole A. Teolis* Josip Lončarić†

Institute for Systems Research
University of Maryland
College Park, MD 20742

Abstract

This research attempts to develop new fundamental knowledge on modeling, design and implementation of control systems for rotary magnetostrictive motors. Well suited for use as direct drive actuators, these motors promise to revolutionize robot technology.

1 Introduction

Growth of dexterity in present robotic manipulators has become stunted by the lack of adequate motor technology. Conventional motors provide inadequate torque, demand excessive power and are in general bulky. Developments in the study of magnetostrictive motors suggest the feasibility of building a rotary electric motor suited for robotic application. The promise of magnetostrictive motors lies in their potential for the realization of low speed/high torque actuation, small power consumption, and compact physical size. Recent advances in the development of magnetostrictive materials indicate potential power densities greater than five times that of present electric motors[13]. Well suited for use as direct drive actuators, these motors promise to revolutionize the field of robotic actuation.

2 Background

Recently linear magnetostrictive motors have been constructed which have met with limited success. Because the technology of magnetostriction is so new, a wealth of analysis and development still needs to be completed. It appears that a rotary motor may be built on the same principle of magnetostriction; however, the design and control of such rotary motors presents new challenges.

*Department of Electrical Engineering and Institute for Systems Research, University of Maryland, College Park, MD 20742. Research supported by NASA Graduate Student Research Program.

†Institute for Systems Research, University of Maryland, College Park, MD 20742. Research supported by NASA grant NAG 5-2029.

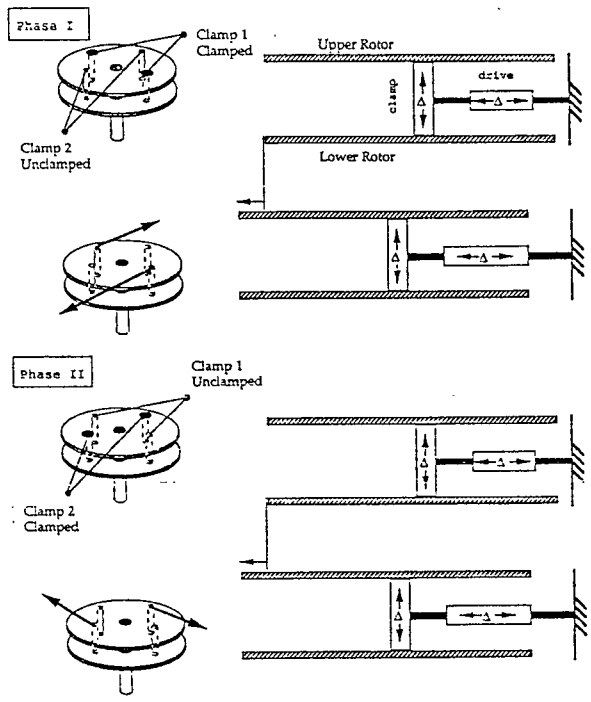

Figure 1: *Motor Operation Cycle*

A rotary motor, using the *giant* magnetostrictive material Terfenol-D, has been designed by John Vranish's team at NASA Goddard and a prototype built. This motor prototype represents the first rotary magnetostrictive motor ever built. Though only in the development stage, the torque outputs of the motor rival torque outputs of the best conventional direct drive motors of the same size available commercially. Hence, there is high potential here for developing a superior direct drive motor. The success of such a project would have significant and long term effects on the progress of robotics.

Initial experiments indicate achievable torques of greater than 10 $ft - lbs$; however, the rotation is exceedingly slow with a maximum of 0.6 rpm. It is expected that by utilizing more sophisticated controllers with optimally shaped control waveforms, both of these figures can be improved.

The basic operation cycle of the rotary motor is depicted in figure 1. As a positive magnetostrictive material, Terfenol-D elongates in the direction of an applied magnetic field. This fundamental property is used as the basis of the drive mechanism in the motor design. Figure 2 shows the *ideal* motions of the terfenol clamp and drive elements. Figure 1 displays only the clamp and drive motions which affect rotor movement during each phase of the cycle.

3 System Model

There are three basic components to the system model: the mechanical/dynamical model, the terfenol model, and the magnetic circuit model(figure 3).

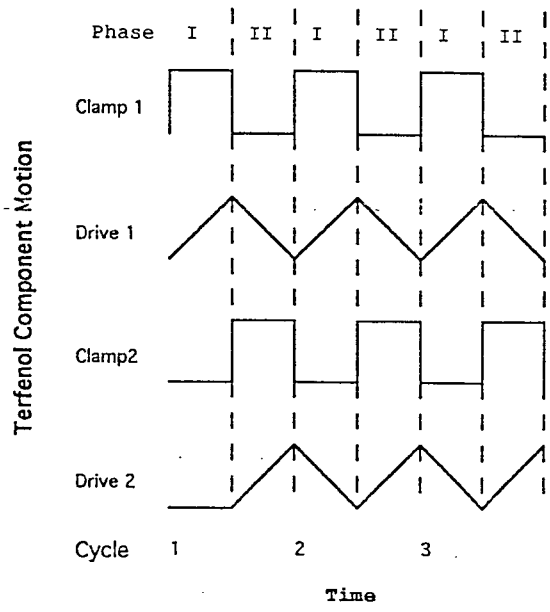

Figure 2: *Ideal Motions of Terfenol Clamp and Drive Elements*

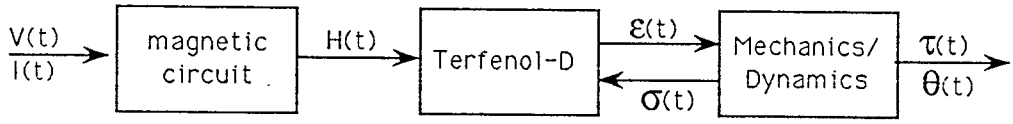

Figure 3: *System Diagram*

The mechanical model and the terfenol model may be developed independently of the magnetic circuit model. The terfenol model does, however, depend on the mechanics of the system. This will be discussed in section 3.2.

At present, no work has been done on modeling the magnetic circuit or trying to estimate the losses. Preliminary calculations have been done to assure that the magnetic field created by the permanent magnets is held essentially constant.

3.1 Mechanical Model

Although terfenol is touted as having the largest room temperature strain of any commercially produced magnetostrictive material, the maximum strain is less than 2×10^{-3} inches per inch.[9] Thus while terfenol is capable of generating hundreds of pounds of force, the corresponding work achieved per cycle is very small; hence high frequency

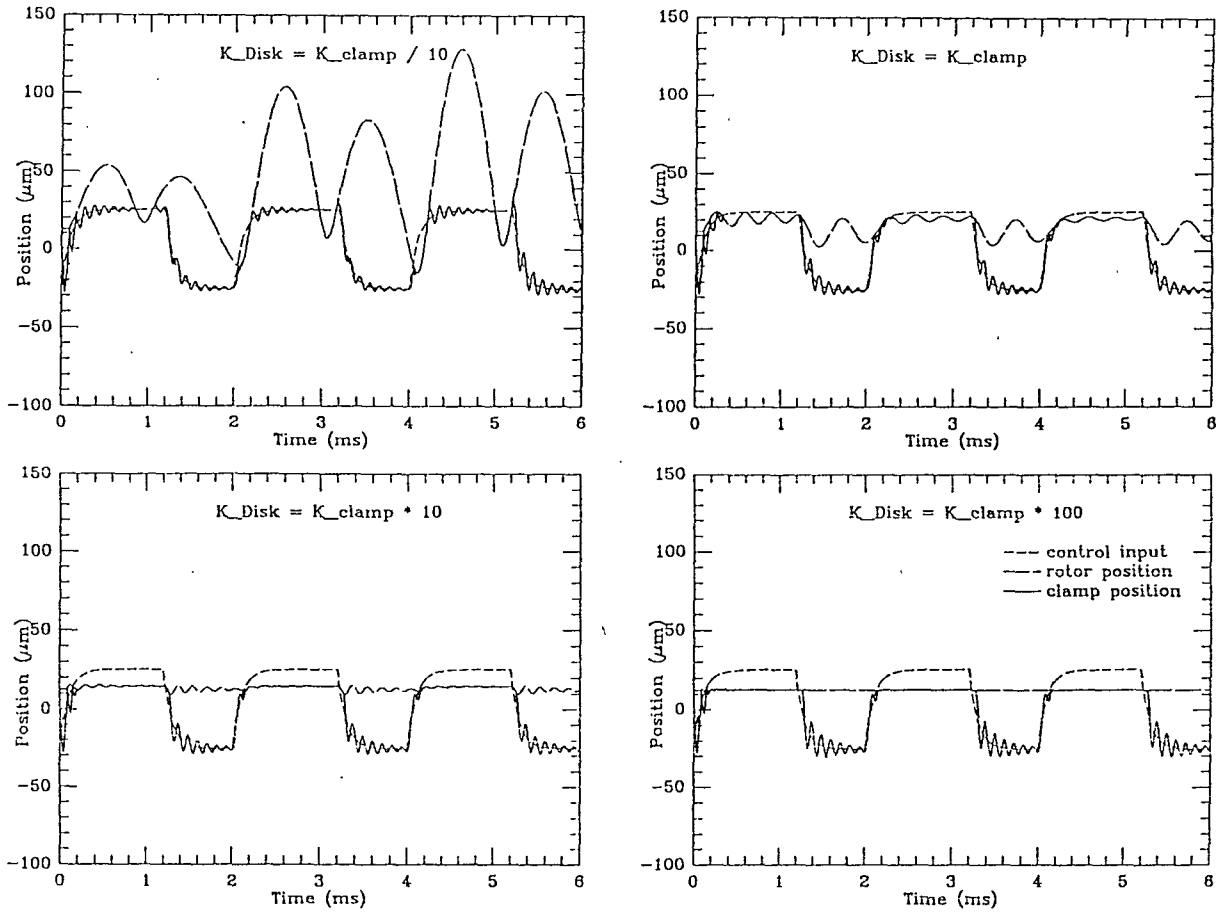

Figure 4: *Simulation Results with Variable Rotor Stiffness*

operation is essential to achieving reasonable power densities. The system should ideally operate at resonant frequency so that a minimum amount of energy will be required.

The high frequency operation, however, will tend to induce unwanted vibrations in the rotor thus making the establishment of a good contact between the clamp and the rotor difficult, if not impossible. With the maximum output torque achievable directly related to the friction between the terfenol clamping assembly and the rotor disk, the importance of this contact is clear. In addition, slippage at this contact may considerably reduce the output speed and torque. By adjusting the elasto-mechanical properties of some components vibrations can be reduced. This is shown in figure 4 as the stiffness of the disk is varied relative to the stiffness of the clamp.

Optimally selecting the shape of the control waveform will also aid in minimizing the vibrations. Having optimally selected the shape and relative phases of the control waveforms for each terfenol component, the operator is left to simply control the velocity and torque by increasing or decreasing the frequency and amplitude respectively of the waveform.

The high frequency cutoff of Terfenol-D is generally due to eddy current losses. The

eddy current causes a power loss and also produces an opposing magnetic field which reduces the effective permeability and inductance. Called the critical frequency, the cutoff increases with decreasing diameter of the terfenol rod. For this design the critical frequency is 1.7 KHz. Motor efficiency may be increased by accounting for the *low pass* nature of the terfenol components when calculating the optimal control input. This has been accounted for in the simulations by using a low pass filtered version of the ideal input. Refer to figures 1 and 4 for descriptions of the ideal input and the simulation input.

3.1.1 Rotor Model

Because of the small motion range of the terfenol components and the necessity for high frequency vibratory operation of the drive mechanism, the elasto-mechanical properties of materials may play a significant role in the control design. A model which accounts for the surface hardness and elastic deformation of critical components is needed.

Careful control of rotor vibrations is important because the vibrations could lead to significant losses. Thus developing a better model for the rotor will be necessary. Further work needs to be done to develop a finite element model of the rotor disk to describe the vibrations and deformations in the disk.

3.1.2 Clamp Model

The maximum output torque achievable, τ_{max}, is directly related to the friction, F_c, between the terfenol clamping assembly and the rotor disk. The exact relation is as follows:

$$\tau_{max} = r\mu F_c \tag{3.1}$$

where r is the radial distance from the output shaft to the clamp and μ is the coefficient of friction of the steel/steel contact.

Because of the importance of the clamping force to torque control, a precise model of the collision of the clamping assembly and rotor is being considered. The coefficient of restitution, R, of the steel/steel contact is about $\sqrt{1/3}$; this indicates that bouncing could be a problem.

Let $\dot{x}$ and $\dot{y}$ denote the velocity of the clamp assembly and velocity of the rotor respectively before collision. Let $\dot{\bar{x}}$ and $\dot{\bar{y}}$ denote the velocities after collision. Then the coefficient of restitution is

$$R = \frac{\dot{\bar{y}} - \dot{\bar{x}}}{\dot{y} - \dot{x}} = \sqrt{1/3} \tag{3.2}$$

Applying the law of conservation of momentum,

$$M_D\dot{y} + M_c\dot{x} = M_D\dot{\bar{y}} + M_c\dot{\bar{x}}, \tag{3.3}$$

the velocities after collision are determined to be

$$\dot{\bar{x}} = \frac{(1-R)M_c\dot{y} + (M_D + RM_c)\dot{x}}{M_c + M_D} \tag{3.4}$$

$$\dot{\bar{y}} = \frac{(1-R)M_D\dot{x} + (M_c + RM_D)\dot{y}}{M_c + M_D} \tag{3.5}$$

component	mass	damping (% critical)	spring constant (N/m)
drive assembly	$M_d = 0.00253\ (kgm^2)$	2.5	$K_d = 9.29x10^4$
clamp assembly	$M_c = 0.0176\ (kg)$	5	$K_c = 2.86x10^7$
rotor	$M_D = 0.1\ (kg)$	5	K_D =???

Table 1: Model Parameters

Both the rotor and the terfenol clamping and driving components have been modeled as underdamped spring-mass systems. The models for the rotor and the clamp respectively before contact are:

$$M_D\ddot{y} + d_D\dot{y} + K_D(y - y_o) = 0 \quad (3.6)$$

$$M_C\ddot{x} + d_C\dot{x} + 2K_Cx = 2K_Cu \quad (3.7)$$

where u denotes the control input to this component: the change in length of the terfenol rod. The estimated model parameters can be found in table 1.

Once a *good* contact has been established, possibly after bouncing, the clamp and the rotor move together according to

$$(M_C + M_D)\ddot{z} + (d_C + d_D)\dot{y} + (2K_C + K_D)y = 2K_Cu + K_Dy_o \quad (3.8)$$

with initial conditions

$$z = x = y \quad (3.9)$$

$$\dot{z} = (M_C\dot{x} + M_D\dot{y})/(M_C + M_D) \quad (3.10)$$

A *good* contact has been made if the following hold:

- $x \geq y$
  Collision has occurred; the clamp and the rotor are touching.
- $\dot{x} \geq 0$ and $\dot{x} \geq \dot{y}$ OR $\dot{x} \leq 0$ and $\dot{x} \leq \dot{y}$
  The rotor is not speeding away from the clamp or visa versa.
- $F = M_D\ddot{z} + d_D\dot{z} + K_D(z - y_o) \geq 0$
  The force between the clamp and the disk is greater than or equal to zero.

The contact is lost when the force between the clamp and the disk diminishes to zero. A block diagram of the simulation algorithm is show in figure 5.

Only weak conclusions can be drawn from the simulations to date since they are based on parameter estimates that could be off by as much as 50%. Although parameter uncertainty constrains the accuracy with which predictions of the motor behavior can be made, critical issues and possible solutions can still be uncovered. For instance, simulation shows that the stiffness of the rotor disk has a significant effect on both (i) control of bouncing between the clamp and the disk, and (ii) oscillations in the disk itself. Simulation also indicates that making the stiffness of the disk at least ten times that of the clamp bouncing and oscillations can be reduced significantly. See figure 4.

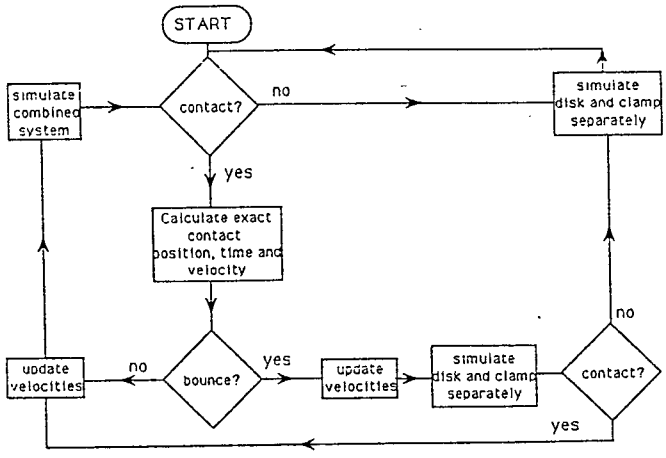

Figure 5: *Clamping Algorithm*

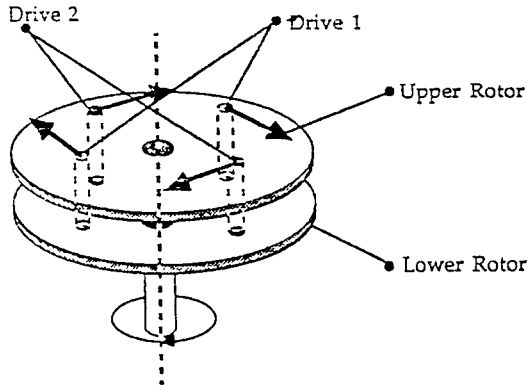

Figure 6: *Driving Mechanism*

3.1.3 Drive Model

The driving mechanism for a rotary magnetostrictive motor is very similar to that of the inch-worm linear motors described by Brockett, Akuta, and Kiesewetter([2] - [10]). These motors use clamp/push operations at high frequency to achieve continuous linear motion. The rotary operation of the NASA motor is similarly achieved by high frequency clamp/push operations. In the rotary case, however, there are four uniformly spaced subsystems which *push* on the rotor tangentially(figure 6).

A state space representation of each of the drive subsystems is as follows:

$$\begin{bmatrix} \dot{x}_1(t) \\ \dot{x}_2(t) \\ \dot{y}_1(t) \\ \dot{y}_2(t) \end{bmatrix} = \begin{bmatrix} 0 & 1 & 0 & 0 \\ -k/m & -d/m & 0 & 0 \\ 0 & 0 & 0 & 1 \\ 0 & 0 & -k/m & -d/m \end{bmatrix} \begin{bmatrix} x_1(t) \\ x_2(t) \\ y_1(t) \\ y_2(t) \end{bmatrix} + \begin{bmatrix} 0 \\ k/m \\ 0 \\ -k/m \end{bmatrix} u(t) \quad (3.11)$$

Again, the control input $u(t)$ is the change in length of the terfenol rods with time. The variable descriptions are given in table 2. Let $\{t_k\}$ denote the sequence of times at which the velocity of the drives, x_2 or y_2, changes direction. Then the net linear displacement

Variable	Description
x_1	position of drive x
y_1	position of drive y
x_2	velocity of drive x
y_2	velocity of drive y
z	net linear displacement
θ	angular displacement
r	radial distance to drive
m	effective rotor mass
k	drive spring constant
d	drive damping

Table 2: Drive System Variable Description

is

$$z(t) = \sum_{\substack{j \text{ odd} \\ j<k}} x_1(t_j) + \sum_{\substack{j \text{ even} \\ j<k}} y_1(t_j) + x_1(t)\ 1(k \text{ odd}) + y_1(t)\ 1(k \text{ even}) \tag{3.12}$$

and the net angular displacement is

$$\theta(t) = \frac{1}{r}\ z(t) \bmod (2\pi r) \tag{3.13}$$

3.2 Terfenol-D Model

The strain, ϵ, in a magnetostrictive material such as Terfenol-D is a function of both magnetic field, H, and compressive stress[1], σ. Consider a terfenol rod with initial strain ϵ_o, stress σ_o, and magnetic field H_o. The total strain may be thought of as the sum[2] of the magnetostrictive strain, ϵ_d, and the mechanical strain, where the mechanical strain obeys Hooke's Law.

$$\epsilon - \epsilon_o = \epsilon_d(H, \sigma) - \frac{\sigma - \sigma_o}{E(H_o)} \tag{3.14}$$

This says that the same total strain will result from first changing the stress alone *then* changing the magnetic field alone as from any other method of reaching the final desired stress and magnetic field. $\Delta\sigma \triangleq \sigma - \sigma_o$ can be written as a function of ϵ; this function will be different for different systems. Observe then that ϵ is a function of itself. This fact makes the problem very difficult to solve analytically. It is thus desirable to formulate a system dependent model for terfenol which relates the total strain to the applied magnetic field taking into account how the stresses change as dictated by the particular mechanical system.

Empirical data for Terfenol-D of the *magnetostrictive strain* versus magnetic field at different fixed stresses[5],[3] are available. Figure 7 displays plots of this data.

[1] Although terfenol is quite strong under compressive stresses, it is very brittle and may break from tensile or shear stresses. Thus we will use stress to refer to compressive stresses unless otherwise indicated.

[2] The strains are small enough that they may be added without significant error.

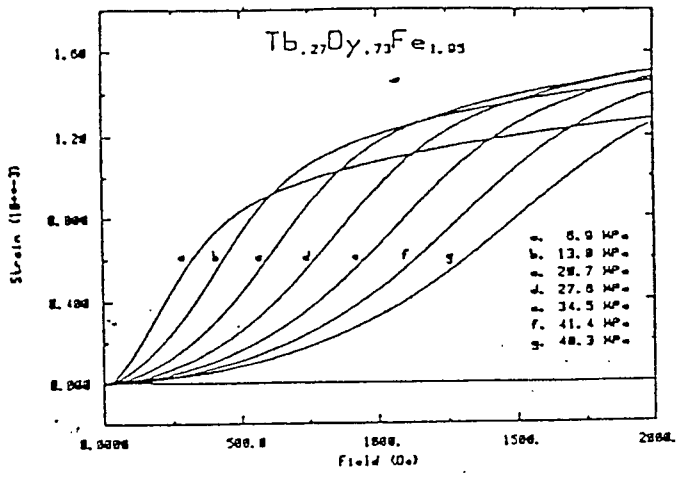

Figure 7: *Magnetostrictive Strain Versus Magnetic Field*[3]

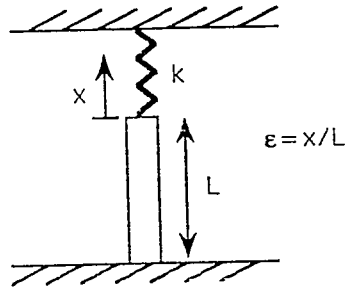

Figure 8: *Terfenol Rod With Compressive Linear Spring*

In most mechanical applications the stress is a nonconstant deterministic function of the strain. For example, if the rotor is modeled as a spring with spring constant k (figure 8). Then the stress on the terfenol clamp as a function of the strain is

$$\Delta\sigma = \frac{kx}{\pi r^2} = \frac{kl}{\pi r^2}\epsilon. \tag{3.15}$$

So as the increased magnetic field increases the clamps strain, the stress is also increased. This causes the total strain on the clamp to be less than predicted by simply considering the magnetostrictive strain at the preload σ_o; this difference could be critical since we are dealing with such small strains.

The problem of finding the total strain versus magnetic field in a terfenol rod has already been examined by Jonas Dyberg[8]. His solution to this problem was to employ a diagram he termed a *universal diagram.* Using the universal diagram, the graph of the functional relation between total strain and magnetic field is found for a particular system. Then a functional approximation to this graph can be found.

The approximation of continuous nonlinear functions is a natural application for

neural networks [4]. It has been shown by Cybenko [7], that continuous functions of finite support may be approximated by a feed forward neural network with a single (finite) hidden layer. It is thus justified that this topology be used here.

4 Research Summary and Future Plans

Work has progressed on developing mechanical models of the motor which are being used to study critical control issues. The clamping process is the source of most of the concern and simulation efforts have been concentrated on this process. Work has begun on simulations which model the drive process and account for possible slipping between the clamp and rotor. Any slippage may considerably reduce the output speed and torque.

A method of modeling the terfenol behavior has been found in [8]. The strain versus magnetic field curve for each of the drive system and the clamp system can easily be found by this graphical method. Once the curves are found, neural networks can be used to approximate the continuous functional relationships.

In addition, work has been initiated on simulation of the motor in a 3D graphical environment. The next step will be to incorporate the models for the terfenol clamps and drives, and eventually the rotor and the magnetic circuit into the graphical simulation. Then with the aid of the graphical simulation, find the controls which maximize motor speed while keeping the rotation smooth.

As evident from the plots in figure 7, compressive stress on the terfenol components can affect their performance and thus the performance of the motor. The compressive stress on the clamps with power off, henceforth referred to as the preset, can easily be adjusted on the prototype. Measurements of velocity and stall torque with both large (high) and small compressive presets were made. Plots of the data are displayed in figure 9. Plots are presented versus the controller clock frequency; there are six clock cycles in each operation cycle.

References

[1] T. Akuta. An application of giant magnetostrictive material to high power actuators. In *Tenth International Workshop on Rare Earth Magnets and Their Applications*, May 1989.

[2] R. W. Brockett. Light weight high performance manipulators. Technical report, US Army Research Office, July 1988.

[3] J. L. Butler. Application manual for the design of EXTREMA Terfenol-D magnetostrictive transducers. Technical report, EDGE Technologies, Inc., February 1988.

[4] A. E. Clark and H. T. Savage. Giant magnetically induced changes in the elastic moduli in $Tb_{.3}Dy_{.7}Fe_2$. *IEEE Transactions on Sonics and Ultrasonics*, 22-1:50–52, January 1975.

[4] An in depth discussion of neural networks is beyond the scope of this paper.

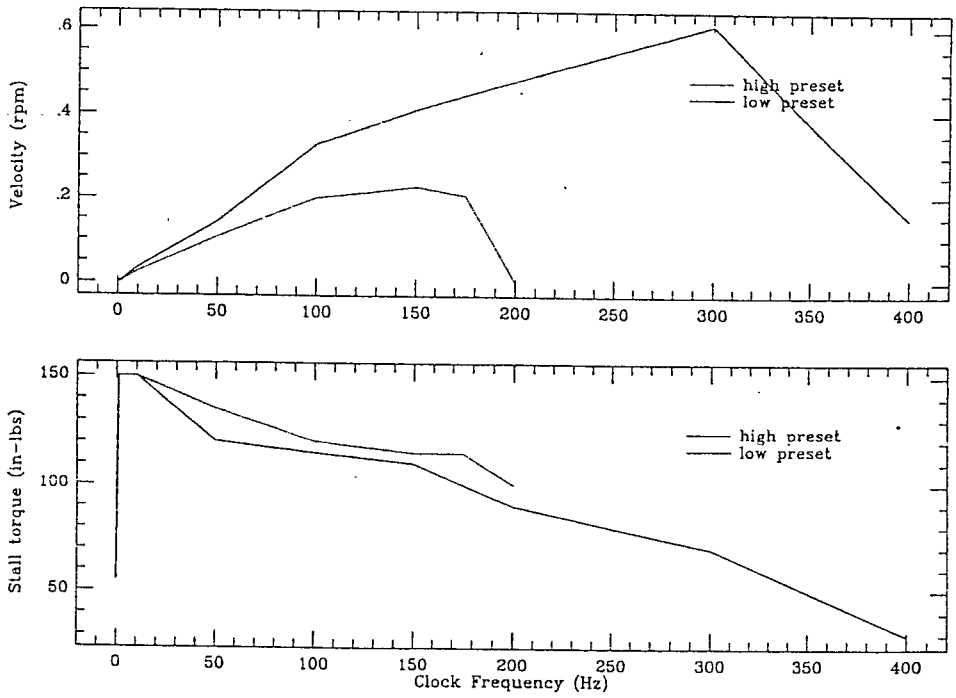

Figure 9: *Velocity and Stall Torque at Different Presets*

[5] A. E. Clark, M. L. Spano, and H. T. Savage. Effect of stress on the magnetostriction and magnetization of rare earth-$re_1.95$ alloys. *IEEE Transactions on Magnetics*, pages 1964–1966, January 1975.

[6] A. E. Clark, J. P. Teter, and M. Wun-Fogle. Magnetical coupling in bridgman-grown $Tb_{.3}Dy_{.7}Fe_{1.9}$ at high drive levels. In *MMM Conference*, November 1989.

[7] G. Cybenko. Approximation by superpositions of a sigmoidal function. Technical report, Tufts University, Department of Computer Science, October 1988.

[8] J. Dyberg. Magnetostrictive rods in mechanical applications. In *The First International Conference on Giant Magnetostrictive Alloys and Thier Impact on Actuator and Sensor Technology*, March 1986.

[9] M. Goodfriend. High strain magnetostrictive alloy for transducers and actuators. *JOM*, page 49, July 1990.

[10] I. L. Kiesewetter. Design guidelines for terfenol actuators. Technical report, Institut fur Feinwerktechnik der TU Berlin, October 1988.

[11] J.L. Meriam. *Dynamics.* John Wiley and Sons, Inc., 1971.

[12] M. Roseau. *Vibrations in Mechanical Systems.* Springer-Verlag, 1987.

[13] J. Vranish. NASA Goddard Space Flight Center. Personal communication.